AE-355
UDC 533.9:621.039.61
536.7:669.791

AE-355

Thermodynamic Analysis of a Supercritical Mercury Power Cycle

A. S. Roberts Jr.

AKTIEBOLAGET ATOMENERGI
STOCKHOLM, SWEDEN 1969

THERMODYNAMIC ANALYSIS OF A SUPERCRITICAL MERCURY POWER CYCLE

A.S. Roberts, Jr.

ABSTRACT

An heat engine is considered which employs supercritical mercury as the working fluid and a magnethydrodynamic (MHD) generator for thermal to electrical energy conversion. The main thrust of the paper is power cycle thermodynamics, where constraints are imposed by utilizing a MHD generator operating between supercritical, electrically conducting states of the working fluid; and, pump work is accomplished with liquid mercury. The temperature range is approximately 300 to 2200°K and system pressure is > 1500 atm. Equilibrium and transport properties are carefully considered since these are known to vary radically in the vicinity of the critical point, which is found near the supercritical states of interest. A maximum gross plant efficiency is 20% with a regenerator effectiveness of 90% and greater, a cycle pressure ratio of two, and with highly efficient pump and generator. Certain specified cycle irreversibilities and others such as heat losses and heat exchanger pressure drops, which are not accounted for explicitly, reduce the gross plant efficiency to a few per cent. Experimental efforts aimed at practical application of the power cycle are discouraged by the marginal thermodynamic performance predicted by this study, unless such applications are insensitive to gross cycle efficiency.

Printed and distributed in April 1969.

LIST OF CONTENTS

1. INTRODUCTION

Performance of a compact plant system utilizing mercury as the working fluid is considered. Gross plant efficiencies are calculated where the objective is to determine the thermodynamic feasibility of a plant constrained to operate with supercritical mercury in a range of thermodynamic states where MHD energy conversion would be possible. Optimum plant performance is not considered.

From a broad view, motivation for the study derives from inherent cycle advantages such as high Carnot efficiency and use of a single-phase fluid and from the realization that the coupling of a MHD pump and generator with an isotopic heat source would yield an high power density plant with no moving parts. Thermal to electrical energy conversion via MHD is interesting because certain fluids, inlcuding mercury, exhibit high electrical conductivity and a gaseous compressibility in a limited domain of supercritical thermodynamic states. The choice of mercury as working fluid is based solely on the availability of supercritical pressure, density, temperature, and electrical conductivity data. Undersea and aerospace auxiliary plant applications are envisaged providing tens of kilowatts electric power output.

A power cycle, operating entirely above the critical pressure of its working fluid, has recently been discussed by Feher [1]. High thermal efficiencies (50-60%) were achieved using carbon dioxide without the MHD constraint confining expansion (work) processes to electrically conducting thermodynamic states. Practical utilization of the supercritical CO_2 cycle is being achieved by Feher in the development of a turbo-generator, Pu^{238} source, space electric power system [2]. A preliminary description of the supercritical mercury-MHD system without regeneration has been written [3], and a brief note [4] outlining regenerative cycle performance has been accepted for publication.

The detailed description of cycle performance is the subject of this report. In section 2. equilibrium and transport properties of the working fluid are presented with special attention given to the supercritical states. Gross cycle efficiency is calculated in section 3. as a function of cycle pressure ratio, unit adiabatic efficiencies, regenerator effectiveness, and generator inlet temperature. Conclusions

are drawn regarding plant feasibility in section 4.

2. THERMOPHYSICAL PROPERTIES OF MERCURY

Thermodynamic data is required for mercury in compressed liquid and supercritical states for power cycle calculations. Liquid P, ρ, T data (pressure, density, temperature) is not readily available for pressures ranging above critical, so recourse to standard state data was necessary [5]. Recent experiments [6, 7, 8], however, have extended the data to include some supercritical states, and the same experiments present electrical resistivity or conductivity data as well.

2.1. Equilibrium Properties

Important deduced properties are gotten from P, ρ, T data; these are enthalpy (h), entropy (s) and specific heats (c_p, c_v). Small letters indicate gram-molar quantities. The deduced properties could be gotten via general thermodynamic relations using an equation of state for the working fluid valid for all states ranging from compressed liquid to supercritical or dense gas states. An equation of state such as,

$$\frac{Pv}{RT} = f(v, T) \qquad (1)$$

does not exist in that range for mercury (R, universal gas constant; $v = 1/\rho$, specific volume). The P, ρ, T data of Kikoin and Senshenkov [8], which cover the range of interest for cycle analysis, was used to generate a two-dimensional fit of the form in equation (1) for supercritical fluid states. However, the deduced properties could not be determined because of the limited accuracy of the data and because of fluctuations induced by the finite degee of the polynomial fits.

In order to determine enthalpy, entropy, and specific heat at constant pressure for the supercritical states, a Van der Waal formalism was employed. As indicated in ref. [3] the Van der Waal equation of state fits the data of Kikoin and Senshenkov [8] satisfactorily in a range where the MHD generator would operate, so that,

$$Z = \frac{Pv}{RT} = \frac{v}{v - b} - \frac{a}{RTv} \qquad (2)$$

where a and be are constants based on the critical state properties from ref. [8], viz.,

$P_c = 1500$ atm $\qquad Z_c = \frac{P_v v_c}{RT_c} = .367$

$v_c = .0352\ \ell/\text{mole}$ (critical compressibility)

$T_c = 1753^{\circ}K$

The Van der Waal constants are found to be,

$$a = 5.64\ \text{atm} \cdot \ell^2 \cdot \text{mole}^{-2}$$

$$b = .001173\ \ell \cdot \text{mole}^{-1}$$

Manipulation of quite general thermodynamic relations yields the folfowing formulae for the deduced properties:

$$h - h_o = \int_{T_o}^{T} c_v d\tau - a\left(\frac{1}{v} - \frac{1}{v_o}\right) + (Pv - P_o v_o) \tag{3}$$

$$s - s_o = \int_{T_o}^{T} c_v \frac{d\tau}{\tau} + R\ \ell n\ \left(\frac{v - b}{v_o - b}\right) \tag{4}$$

$$c_p - c_v = \frac{R}{1 - \frac{2a(v-b)^2}{RT\,v^3}} \tag{5}$$

$$c_v = c_v^o(T) \tag{6}$$

This set of equations includes the caloric relations for the generator process in the power cycle; $c_v^o(T)$ is an ideal gas specific heat function (see ref. [3]), unknown for the high temperature mercury. However, assuming an ideal, monatomic gas *), $c_v^o = 3/2 \cdot R$, so that equations (3)-(5) completely specify the properties from any

*) A valid assumption away from the critical point since polymerization (clustering of molecules) effects are probably important there [14].

initial state (P_o, v_o, T_o) so long as the fluid is homogeneous (single-phase) throughout the region of integration.

For the liquid states there is no general state equation; consequently, enthalpy is defined as,

$$h - h_o = \langle c_p \rangle (T - T_o) \tag{7}$$

where

$$\langle c_p \rangle = \frac{\int_{T_o}^{T} C_p d\tau}{\int_{T_o}^{T} d\tau} \qquad \text{along an isobar.}$$

The pressure dependence of c_p was neglected for $T \lesssim 1000^{\circ}K$, and handbook values at 1 atm were used [5]. Liquid entropies were not calculated. The deduced values of specific heat at constant pressure used in the cycle calculations are graphed in figure 1 showing temperature and pressure dependence. A sharp rise is noted in c_p as critical temperature and pressure are approached in qualitative agreement with theory and experiment [9]. There is, however, some controversy regarding the extent of extrema of certain properties in the vicinity of the critical point and regarding the locii of extrema [10]. Cognizance must be taken of these variations in equilibrium properties since states of the supercritical power cycle are found near the critical point. The sonic speed is another parameter the variation of which is important for MHD generator calculations. Using equation (2) and (4) the sonic speed, a_s, can be estimated from the definition

$$a_s^2 = - v^2 \left(\frac{\partial P}{\partial v}\right)_s$$

a typical value at $T = 2023^{\circ}K$, $v = .0222\ \ell \cdot mol^{-1}$ is $a_s = 940$ m/sec. It is expected that the supercritical MHD generator would operate in the subsonic range (see ref. [4]).

2.2. Transport Properties

Of the several properties pertinent to the generator work process, electrical conductivity and viscosity were studied. Some electrical conductivity data exist, but no viscosity values were found at the required temperature and pressures.

The measured resistivities of Kikoin and Senshenkov [8] are preferred, because the range of the data is greater. It is noted that comparison of resistivity values between experiments [8] and [6] is not particularly good although the conducting-non-conducting transition is clearly indicated in either case. The data of ref. [8] is inverted to produce a conductivity (σ) plot in figure 2. A graph of σ/σ_o vs. T is made with pressure as the parameter; the range of T and P corresponds to states of interest during generator work processes. The conductivity transition is spectacularly indicated with σ/σ_o changing by five (5) orders of magnitude along some isobars in a temperature span of 250°K. The general orientation of the conductivity transition is shown on an h-s diagram in figure 4.

In the absence of experimental data for viscosity, calculational methods from kinetic theory are employed. A formula [9] for absolute viscosity of dilute gases,

$$\eta_o = \frac{2.67 \times 10^{-5} (MT)^{1/2}}{\bar{\sigma}^2 \Omega(2,2)^*} \qquad |gm \cdot cm^{-1} \cdot sec^{-1}| \qquad (8)$$

has been shown to correlate with mercury data [11] at ordinary pressures and to a temperature of 1400°K.

M, molecular weight

$\bar{\sigma}$, molecular collision diameter, Å

$\Omega^{(2,2)^*}$ transport integral from [9]

T, absolute temperature, °K

The Enskog technique [9] extends the calculation to dense fluid states when P, v, T data are available. The following equations are used:

$$\left(\frac{\eta}{\eta_o}\right)\left(\frac{v}{b_o}\right) = \frac{1}{y} + .8 + .7614\, y \qquad (9)$$

$$y = \frac{v}{RT}\left\{T\left(\frac{\partial P}{\partial T}\right)_v\right\} - 1 \qquad (10)$$

The parameter b_o is determined by noting that

$$vy \to b_o$$

as

$$\rho = 1/v \to 0$$

since $\rho \to 0$ is a condition for existence of an ideal gas state for which $\eta = \eta_o$. Under this necessary condition equation (9) reduces to $\eta/\eta_o = 1$; b_o takes different values as a function of temperature. The method has been successfully tested for N_2 and CO_2 [12] and for ethane [13], although it is based on an idealized theory of dense fluids. This method is applied using the mercury data of ref. [8], and consistent correlation results over a limited range of temperature and pressure; η/η_o is graphed in figure 3. The slope of the isotherms appears correct since $\eta/\eta_o \to 1$ at low pressures. A new result is that the viscosity of supercritical mercury is a factor of 20-70 times the viscosity at ordinary pressures and that a non-linear temperature dependence indicates a rapid increase in η as critical temperature is approached from above. The effect of viscosity on a MHD generator analysis has been considered qualitatively in ref. [4], where it is argued that inertial forces still dominate flow behaviour.

3. POWER CYCLE PERFORMANCE

The performance criterion, to be defined below, is the gross plant efficiency. Basically it measures the internal energy conversion efficiency of the cycle up to the therminals of the generator and is a ratio of net work done to heat rate at the source. Basic assumptions used throughout are, (1) all piping and components other than heat exchangers are adiabatic, (2) there are no extraneous heat losses from the heat exchangers, and (3) frictional pressure drop is neglected in piping and heat exchangers. However, real dissipative effects are allowed in pump and generator. Finally, magnet excitation if required is not charged to the cycle.

3.1. Plant Description

The regenerative, supercritical power cycle is depicted in figure 4. Starting at the generator exhaust condition in figure 4a, the process 1'a transfers heat to the high pressure fluid in the regenerator, process 1'a2 rejects heat to the surroundings, process 23a represents adiabatic pump compression, process 3a3'a is isobaric heat addition in the regenerator, process 3'a4a is isobaric heat addition from the source, and finally process 4a1 is the adiabatic expansion process in the generator. The enthalpy decrease, $(h_{4a} - h_1)$ measures the thermal energy converted to gross electrical work, a portion of which must drive the pump. Use of the regenerative heat exchange allows recuperation of generator exhaust energy at high temperature providing an improved gross cycle efficiency by reducing the required energy input from the source. From another view the effect is to lower the temperature at which heat is rejected thereby improving the Carnot efficiency. The regenerative cycle appears more useful when it stands alone relative to the case where the supercritical MHD cycle is used as a topping unit, but final assessment of topping performance would require a new study defining a dual cycle plant.

Exhaust energy is recovered in a regenerator, but also temperature is "recuperated". The final limit on the degree of regeneration is defined when the temperature of the high pressure fluid entering the source approaches the temperature of the low pressure fluid exiting the generator, i.e., when $T_{3'a} = T_1$ in figure 4. A prohibitively large heat transfer surface in the regenerator is required to achieve this condition. Useful measures of regenerator effectiveness are,

$$\eta_{reg}(\text{energy}) = \frac{h_{3'a} - h_{3a}}{h_1 - h_{3a}} \tag{11}$$

$$\eta^{T}_{reg}(\text{temperature}) = \frac{T_{3'a} - T_{3a}}{T_1 - T_{3a}} \tag{12}$$

also the "pinch" temperature across the regenerator,

$$\Delta T_{pinch} = T_1 - T_{3'a} > 0 \tag{13}$$

No more detailed definition of regenerator design and function is required for initial cycle calculations.

3.2. Range of Operating Parameters

At pressures such that $P > P_{crit}$ the working fluid experiences a continuous phase transition in the power cycle, so for mercury $P > 1500$ atm. Other fluids such as mercury-alkali metal amalgams and ammonia-alkali metal solutions, for which data is limited, have high electrical conductivities and more desirable critical pressures ranging only a few hundred atmospheres. Mercury has the lowest critical temperature of the low-melting metals, $T_{crit} = 1753^{\circ}K$, and in the power cycle temperatures range $373\text{-}2300^{\circ}K$.

The power cycle is located in a field of thermodynamic states by fixing the position of state point 1 in figure 4. This is achieved by placing the generator process as far into the "gas" region as is consistent with a high electrical conductivity. One desires simultaneously low T and P but high v and σ. Thus the coordinates of state point 1 are assigned as $T_1 = 1926^{\circ}K$, $P_1 = 2600$ atm; the electrical conductivity (at generator exhaust) is found as $\sigma_1 = 3000$ ohm$^{-1} \cdot$ m^{-1} from figure 2, increasing by about an order of magnitude at state point 4a (generator inlet). The generator process is idealized here to include aperfect nozzle and diffuser. The cycle pressure ratios are kept low in consideration of the pump and the already high system pressures, i.e., $P_4/P_1 < 2.5$. Changes in specific heats are inherently accounted for through calculation of enthalpy differences. Only enthalpy differences are of concern for efficiency calculations, so arbitrary reference values of enthalpy and entropy (where needed) were assigned at state point 1. The Van der Waal model provides a reliable means of calculating state properties so long as $\rho \lesssim 10$ gm/cm^3 or $v \gtrsim .020$ ℓ/mol for supercritical states; this was ascertained by comparison with the data of ref. [8].

3.3. Efficiency Calculations

Gross cycle efficiency is defined by considering the process of converting thermal power at the source to electrical power at the generator, so that,

$$P(el) = \eta_{el} \cdot \eta \cdot P(th) \qquad (14)$$

where η_{el} is an efficiency of external auxiliary equipment and η is the gross cycle efficiency. The internal definition of η calls for a subdivision,

$$\eta = \frac{w^a_{net}}{q_{in}} = \frac{w^a_{net}}{w_{net}} \cdot \frac{w_{net}}{q_{in}} \tag{15}$$

where w_{net} is the ideal, net cycle work done via isentropic processes, w^a_{net} is the net cycle work done in actual processes, and q_{in} is the heat added at the source all written per gram-mole of working fluid. By referring to figure 4a the above quantities can be written in terms of enthalpy differences where,

$$\left.\begin{aligned} w_{net} &= (h_4 - h_1) - (h_3 - h_2) \\ w^a_{net} &= (h_{4a} - h_1) - (h_{3a} - h_2) \\ q_{in} &= (h_{4a} - h_{3'a}) \end{aligned}\right\} \tag{16}$$

for the regenerative cycle. Substituting into equation (15) there obtains,

$$\eta = \frac{1 - \dfrac{(1 - W_R)}{\eta_{ip}\,\eta_{ig}}}{1 + \dfrac{1}{\eta_{ig}}\left(\dfrac{h_1 - h_{3'a}}{h_4 - h_1}\right)} \tag{17}$$

with the usual pump and generator isentropic efficiencies,

$$\eta_{ip} = \frac{h_3 - h_2}{h_{3a} - h_2} \tag{18}$$

$$\eta_{ig} = \frac{h_{4a} - h_1}{h_4 - h_1} \tag{19}$$

and a work ratio, W_R, defined as

$$W_R = \frac{w_{net}}{w_{gen}} = \frac{(h_4 - h_1) - (h_3 - h_2)}{(h_4 - h_1)} \tag{20}$$

The enthalpy difference ratio in the denominator of (17) is another

measure of regenerator performance, being the fraction of ideal generator work not recuperated from generator exhaust energy; the effectiveness parameters of equations (11), (12), and (13) are preferred since they are more often found in the literature.

Three independent bits of information are required in order to calculate η from equation (17). The isentropic efficiencies are selected to reflect performance of pump and generator; equilibrium state points for the ideal cycle are calculated to specify ideal enthalpies and W_R; and, a regenerator effectiveness is chosen to represent reasonable performance of this heat exchanger. With the reference state point already selected (1 in figure 4a), T_4 or P_4 and T_2 are assigned values of interest. The remaining ideal cycle state properties are then calculated based on equations (3) - (6) and the liquid data. A set of independently chosen parameters includes: P_4, T_2, η^T_{reg}, η_{ip}, and η_{ig}. The pressure ratio is determined and as implied in figure 4a, $P_4/P_1 = P_3/P_2$ since $P_1 = P_2$. All that remains is to present the results of a parametric study.

Figure 5 is a graph of η vs. P_4/P_1 with regenerator effectiveness as the parameter. There is a strong parametric influence; these are not high performance regenerators, and ΔT_{pinch} would be undesirably high. The pump inlet temperature $T_2 = 373^oK$, is established since a calculation at $T_2 = 273^oK$, $P_4/P_1 = 2.18$ showed a negligible improvement in η. In figure 5, η is termed the "ideal" gross plant efficiency since pump and generator performance is isentropic and adiabatic.

With perfect regeneration, $\eta^T_{reg} = 1$, $\Delta T_{pinch} = 0$, figure 6 contrasts the effect of varying separately pump and generator isentropic efficiencies. It is clear that even under these optimistic circumstances, that it is necessary for $(\eta_{ip}, \eta_{ig}) > .6$ to achieve net output. It is further noted that variation in η_{ip} or η_{ig} has approximately equal effect on η; this indicates that the numerator of equation (17) is controlling, so that η is strongly dependent on the work ratio, W_R, which tends to be low for the mercury MHD-supercritical cycle [4].

Again in figure 7 cycle pressure ratio is the independent variable, and the effect on η of different values of η_{ig} is observed. Some practical consideration is given here to reasonable values of pump and generator parameters; $\eta_{ip} = .9$ is chosen since that value is achievable

for mechanical pumps, and the pinch temperature is set at $10^{o}K$ producing a relatively high degree of temperature and energy recuperation. A similar result is plotted in figure 8, where now the independent variable is generator inlet temperature, T_{4a}.

These results show generally that η is an increasing function of P_4/P_1, T_{4a}, η_{ip}, η_{ig}, and η^{T}_{reg} except under the circumstances where $\eta_{ig} \leq .7$; then $\eta \sim 3\%$ independent of T_{4a} and P_4/P_1 beyond $P_4/P_1 = 1.2$, the remaining parameters being fixed.

3.4. Kw(el) Output

Based on the above analysis an estimate of electric power can be made for this non-optimal system. From equation (14),

$$P(el) = \eta_{el} \cdot \eta \cdot P(th)$$

$$= (.9)(.2)\, P(th)$$

The value η_{el} is attainable, and η is an optimistic value from this study. Five to fifty Kw(th) have been suggested [3, 2] as the thermal power convected away from the heat source. The estimates were qualitatively based on consideration of pump capability, heat exchanger characteristics, and use of an isotopic heat source. With these values a range for maximum power output, based on the stipulated ground-rules, is,

$$P(el) = .9 - 9.0 \text{ (Kw(el)}$$

4. SUMMARY AND CONCLUSIONS

Optimistic values of η_{ip} and η_{ig} are presumed in this study in order to achieve a gross cycle efficiency of 20% or slightly greater. Mechanical pumps often have an isentropic efficiency of 90%, but values of 20% are more realistic for electromagnetic pumps [15]. So, the price payed for no moving parts could be no net power (see figure 6). Also, in the physically simple MHD generator it is difficult to achieve isentropic efficiencies as great as 80%. These problems of unit efficiency would be less significant if η were improved by increasing W_R, the ratio of i-

deal net cycle to gross generator work, i.e., values of η are strongly limited by the desire to keep the generator process in a region of dense, conducting gas states, where unfortunately expansion work is minimal. It is felt that gains made from optimizing heat exchanger design and the coupling between components would be insignificant after allowing for loss mechanisms such as pressure drops and thermal leakage.

The possibility of finding other working fluids with significantly improved thermodynamic characteristics must be emphasized. As noted earlier there is a wide spectrum of fluids which exhibit the metal-nonmetal transition and often at much lower temperatures and pressures relative to mercury. Experimental work to determine equilibrium and transport properties of fluids adaptable for supercritical power cycles is essential. Flow properties could be examined in a small supercritical test loop; or, a low pressure and temperature experimental model might provide hydrodynamic and electric similitude. Some further analytic work is needed immediately to specify MHD generator performance and values for η_{ig}; a compact, axial B-field vortex generator has intuitive appeal in conjunction with the supercritical power cycle.

Liquid metal technology is advancing rapidly, so that electromagnetic pumps have been operated at temperatures of $1000^{\circ}K$ and higher [16] with pressure of a few bars. However, the extrapolation to $2000^{\circ}K$ and pressures of several thousand bars is difficult even in a compact prototype. High strength refractory metal alloys must be employed [17] implying expensive experimental design. Although there are many intriguing analytical aspects of the supercritical MHD system and some conceivable applications, the marginal thermodynamic performance of the power cycle together with obvious technological difficulties discourages system prototype development in the near future.

ACKNOWLEDGEMENT

The author wishes to recognize the able technical assistance provided by Mr. Stanley Svensson in programming the cycle calculations for the digital computer and Mr. Odd Olofsson for computational work and data presentation.

REFERENCES

1. FEHER E.G.,
The supercritical thermodynamic power cycle.
Energy conversion 8 (1968) p. 85.

2. FEHER E.G.,
Application of the supercritical cycle to electric power generation in space.
3. Intersociety energy conversion eng. conf., Boulder, Colo., Aug. 13-16, 1968. (Douglas paper 4932)

3. ROBERTS A.S. Jr.,
1968. AB Atomenergi, Sweden.
(Internal report FFA-833.)

4. BRAUN J. and ROBERTS A.S. Jr.,
A supercritical thermodynamic power cycle with MHD generator.
To be published in the AIAA journal early 1969.

5. LYON R.N. (Ed.),
Liquid metals handbook. 1952.
(NAVEXOS-P-733 (Rev.)).

6. FRANCK E.U. and HENSEL F.,
Metallic conductance of supercritical mercury gas at high pressures.
Phys. Rev. 147 (1966) p. 109.

7. POSTILL D.R., ROSS R.G. and CUSACK N.E.,
Equation of state and electrical resistivity of liquid mercury at elevated temperatures and pressures.
Advan. Phys. 16 (1967) p. 493.

8. KIKOIN I.K. and SENSHENKOV A.P.,
Electrical conductivity and equation of state of mercury in the temperature range 0-2000°C and pressure range of 200-5000 atm.
Phys. metals metallogr. 24 (1967):5 p. 74.

9. HIRSCHFELDER J.O., CURTISS C.F. and BIRD R.B.,
Molecular theory of gases and liquids.
John Wiley & Sons Inc., New York 1954.

10. GITERMAN M.Sh.,
Behaviour of matter in the supercritical region.
High temp. 5 (1967) p. 224.

11. SHINS H.E.J.,
Liquid metals for heat-pipes, properties, plots and data sheets. 1967.
(EUR 3653 e)

12. BIRD R.B., HIRSCHFELDER J.O. and CURTISS C.F.,
The equation of state and transport properties of gases and liquids. Pt. 5. Chap. 4 in Handbook of physics. 2 ed.
Eds. E.U. Condon and H. Odishaw.
Mc Graw-Hill, New York 1967, p. 5-45.

13. HAMRIN C.E. Jr. and THODOS G.,
Reduced state correlation for the Enskog modules developed from PVT data for ethane.
J. chem. eng. data 13 (1968) p. 57.

14. HENSEL F. and FRANCK E.U.,
Metal-nonmetal transition in dense mercury vapor.
Rev. mod. phys. 40 (1968) p. 697.

15. DIEDRICH G.E. and GAHAN J.W.,
Design of two electromagnetic pumps. 1967.
(NASA-CR-911)

16. PORTE D.,
MHD en phase liquide et technologie des metaux alcalins.
Rev. gén. de l'électricité 76 (1967) p. 923.

17. Tungsten alloy has improved ductility.
Mech. eng. 90 (1968):9 p. 59.

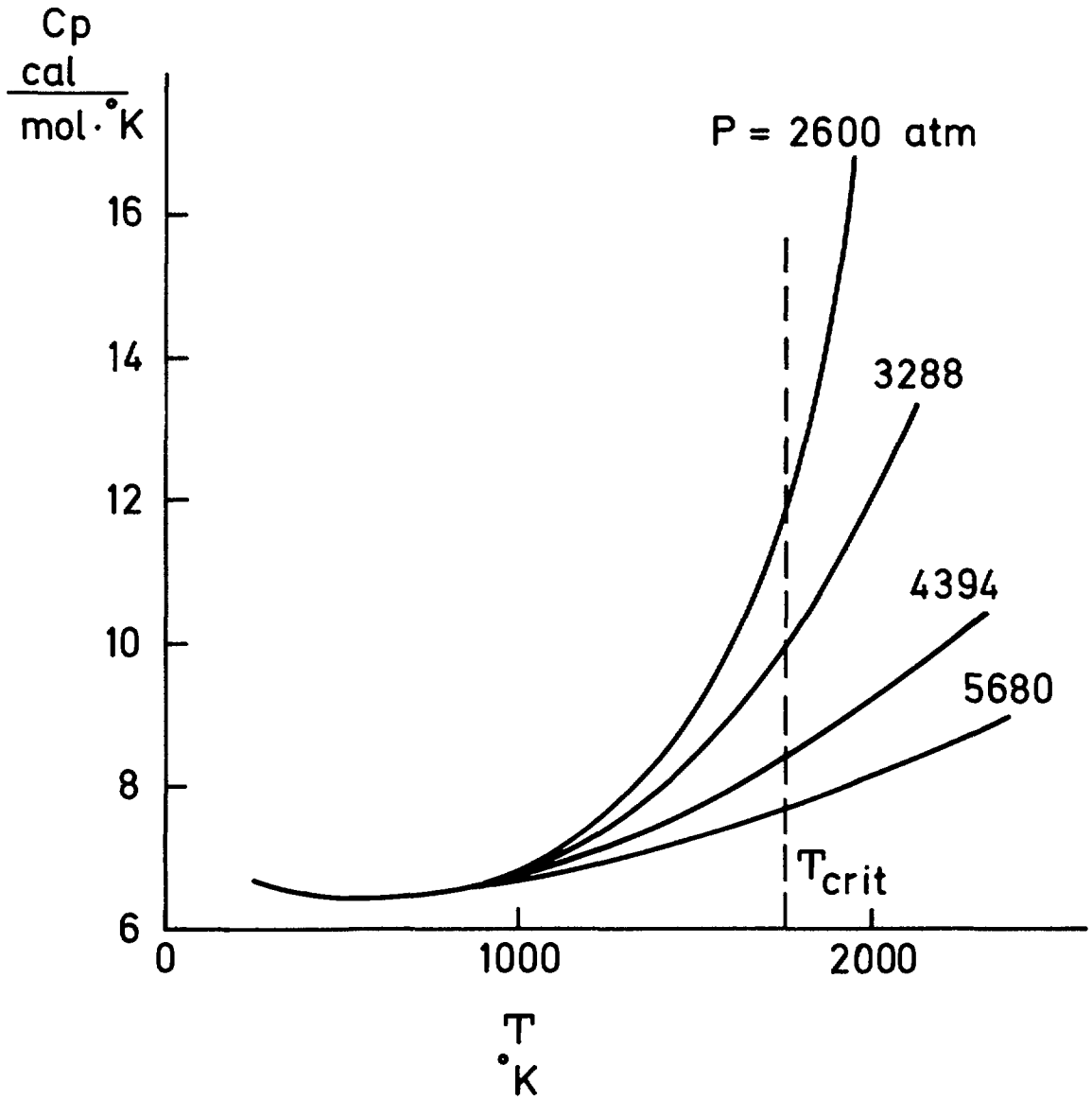

Fig. 1 Values of Cp for mercury deduced from van der Waal model and data tabulations

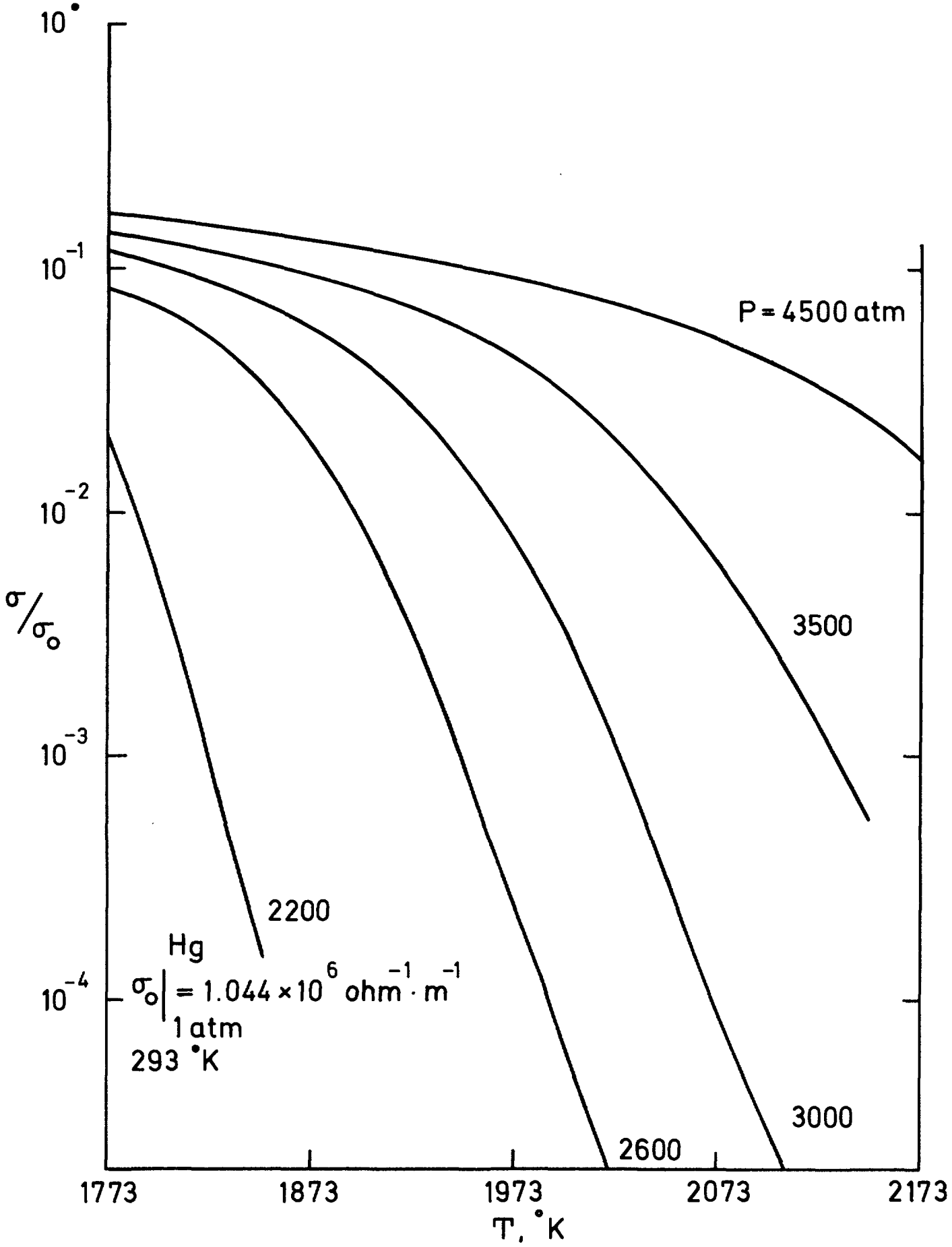

Fig. 2 Electrical conductivity ratio of Kikoin and Senshenkov [8]

η_o $\left(\frac{gm}{sec \cdot cm}\right)$	T (°K)
0.001323	1923
0.001386	2023
0.001448	2123

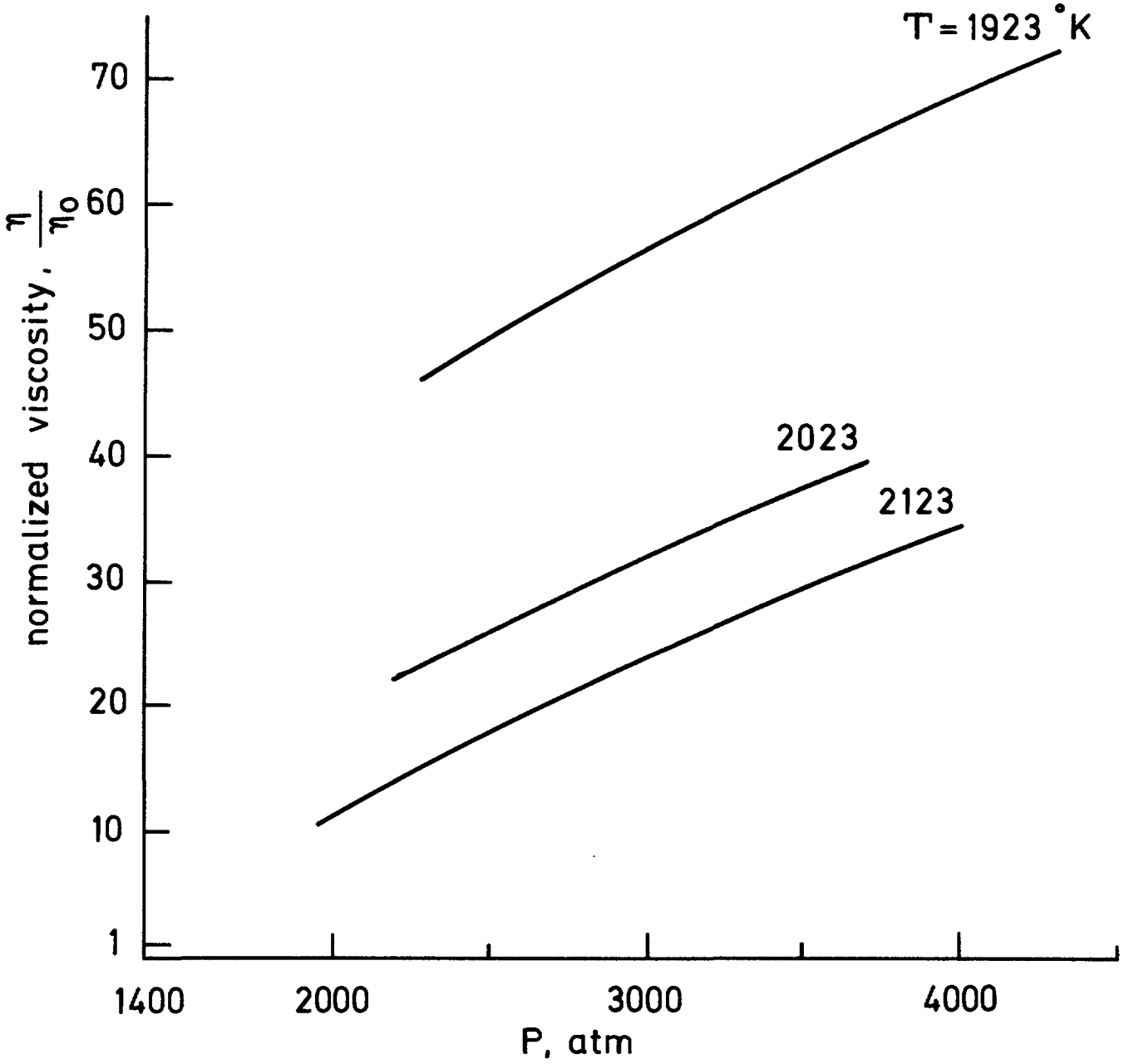

Fig. 3 Viscosity via Enskog technique from graphical values of $\left(\frac{\delta P}{\delta T}\right)_v$ derived from data of [8]

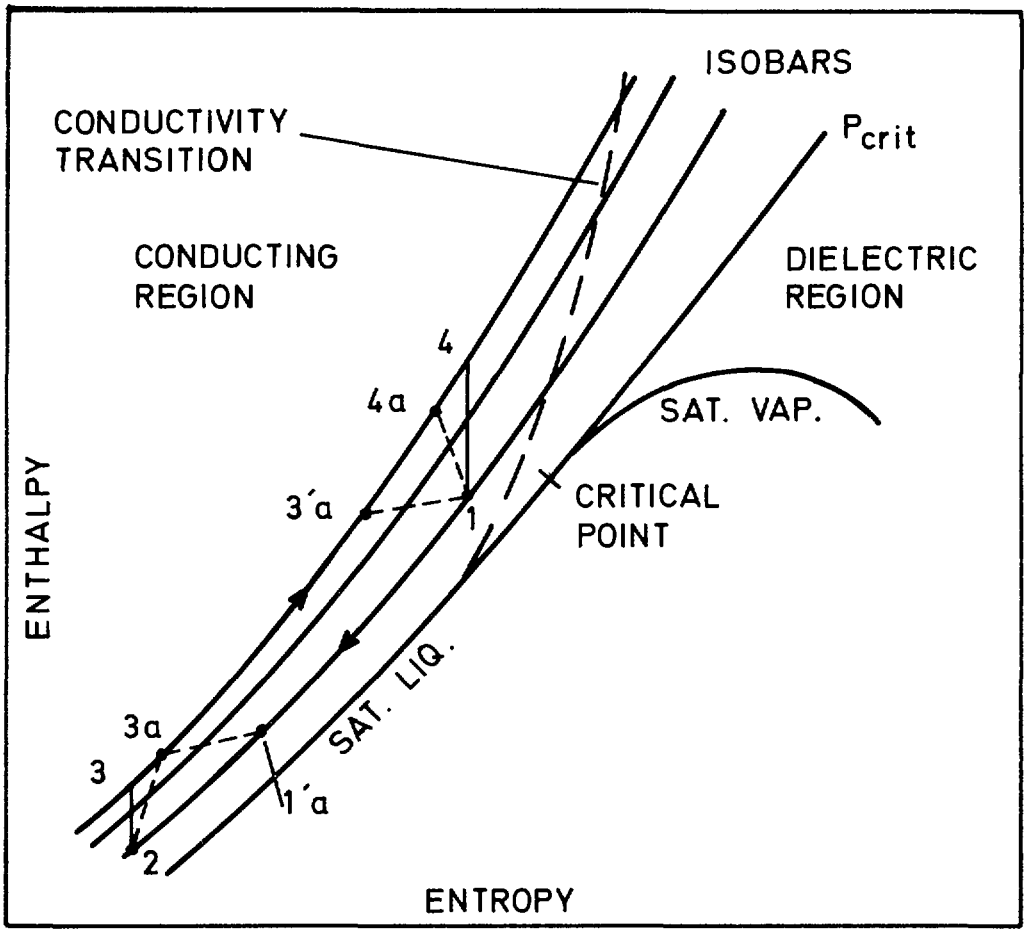

Fig. 4a

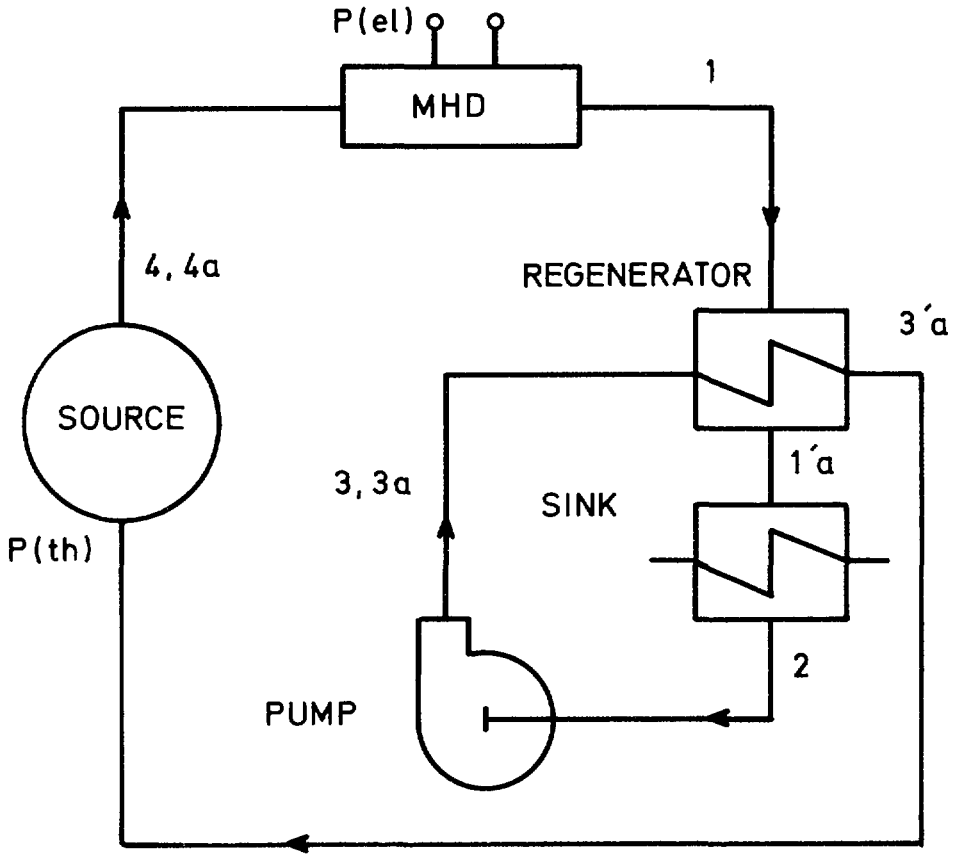

Fig. 4b

Fig. 4 Cycle diagram and plant schematic

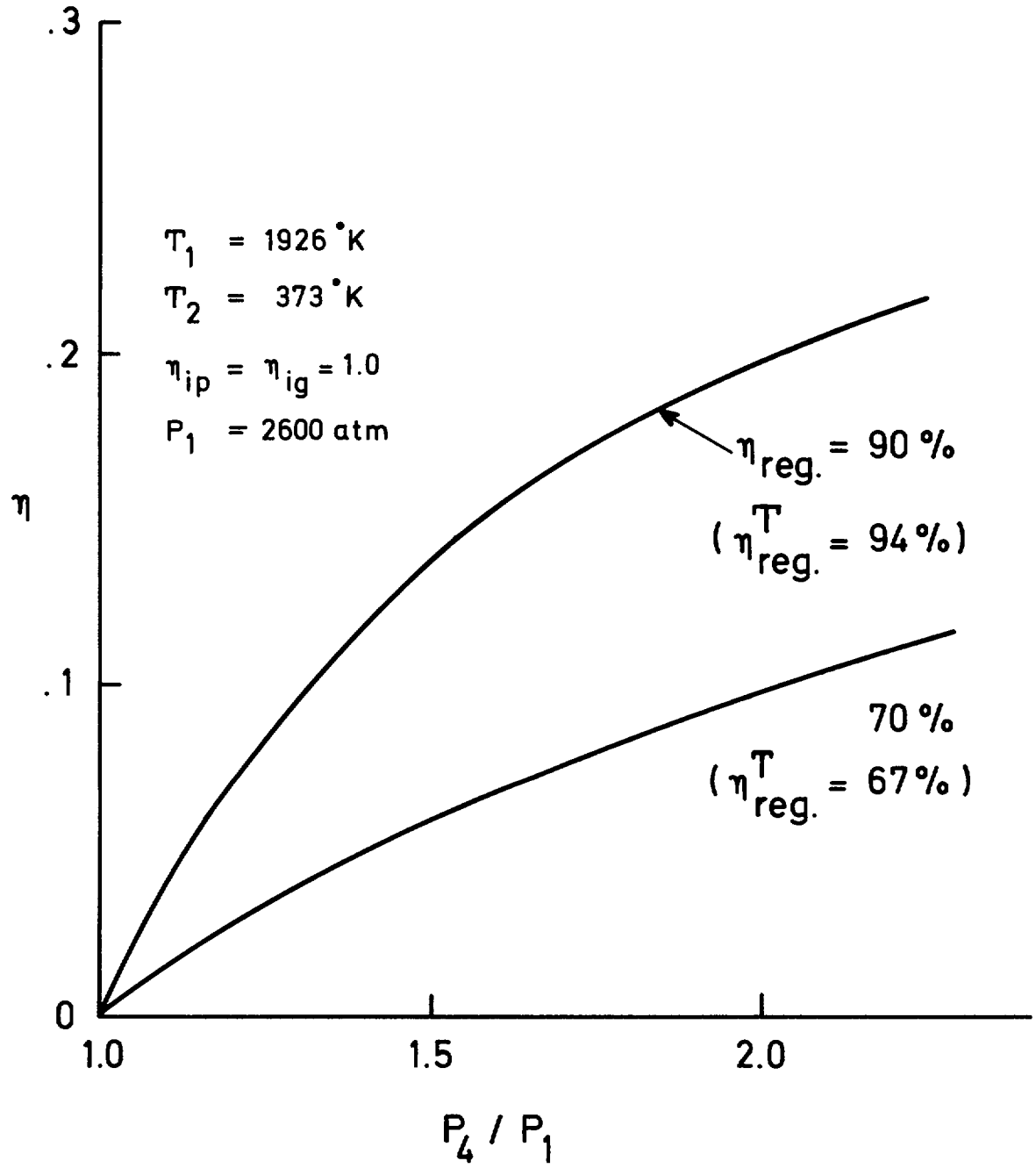

Fig. 5 Ideal gross plant efficiency with percent regeneration as parameter

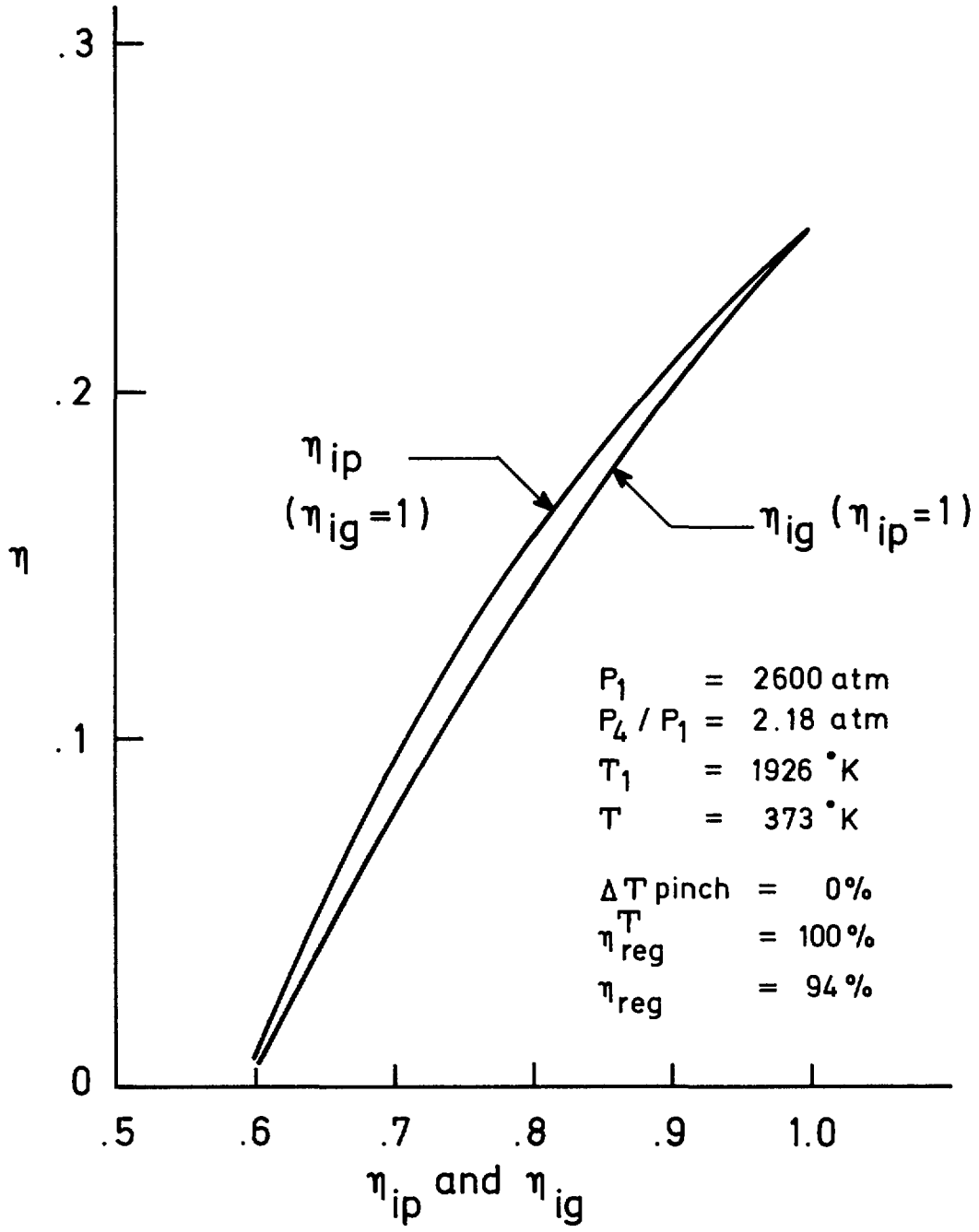

Fig. 6 Effect of unit isentropic efficiencies on gross plant efficiency

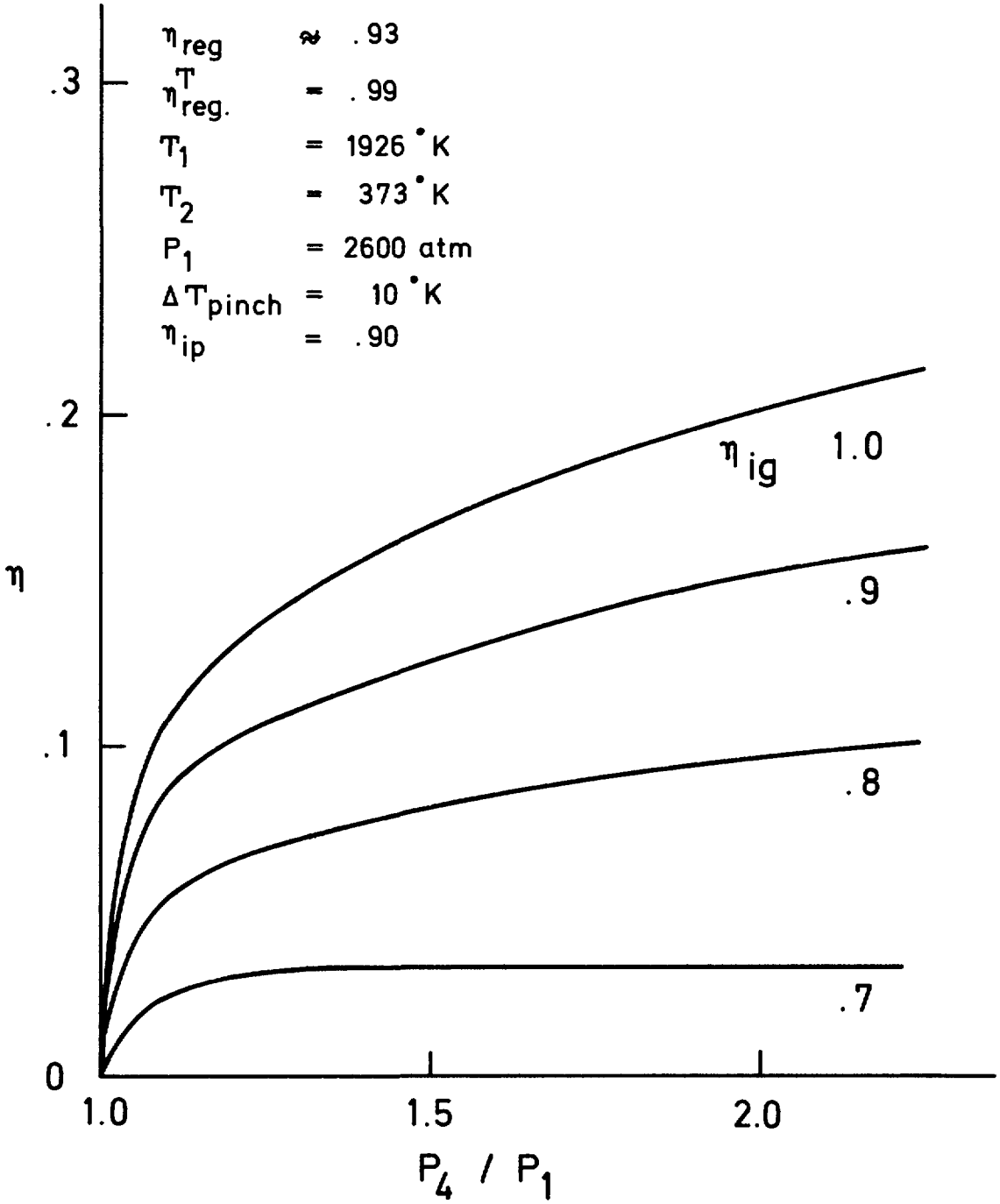

Fig. 7 Gross plant efficiency versus ratio and η_{ig}

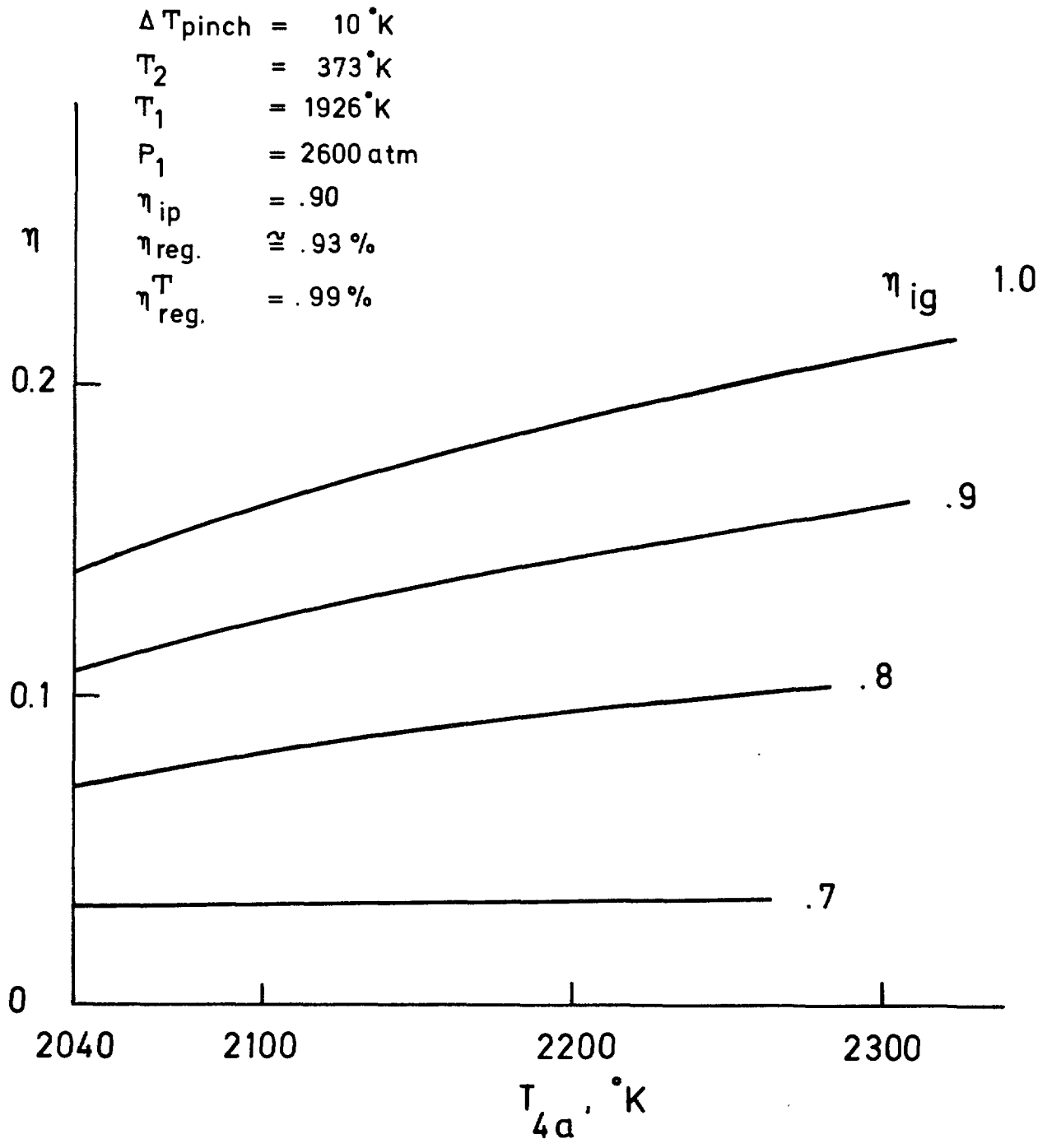

Fig. 8 Gross plant efficiency versus inlet temperature and η_{ig}

LIST OF PUBLISHED AE-REPORTS

1–280. (See the back cover earlier reports.)

281 Collision probabilities for finite cylinders and cuboids. By I. Carlvik. 1967. 28 p Sw. cr. 10:–.

282. Polarized elastic fast-neutron scattering of ^{12}C in the lower MeV-range. I Experimental part. By O. Aspelund. 1967. 50 p. Sw. cr. 10:–.

283. Progress report 1966. Nuclear chemistry. 1967. 26 p. Sw. cr. 10:–.

284. Finite-geometry and polarized multiple-scattering corrections of experimental fast-neutron polarization data by means of Monte Carlo methods. By O. Aspelund and B. Gustafsson. 1967. 60 p. Sw. cr. 10:–.

285. Power disturbances close to hydrodynamic instability in natural circulation two-phase flow. By R. P. Mathisen and O. Eklind. 1967. 34 p. Sw. cr. 10:–.

286. Calculation of steam volume fraction in subcooled boiling. By S. Z. Rouhani. 1967. 26 p. Sw. cr. 10:–.

287. Absolute E1, $\Delta K = 0$ transition rates in odd-mass Pm and Eu-isotopes. By S. G. Malmskog. 1967. 33 p. Sw. cr. 10:–.

288. Irradiation effects in Fortiweld steel containing different boron isotopes. By M. Grounes. 1967. 21 p. Sw. cr. 10.

289. Measurements of the reactivity properties of the Ågesta nuclear power reactor at zero power. By G. Bernander. 1967. 43 p. Sw. cr. 10:–.

290. Determination of mercury in aqueous samples by means of neutron activation analysis with an account of flux disturbances. By D. Brune and K. Jirlow. 1967. 15 p. Sw. cr. 10:–.

291. Separtaion of ^{51}Cr by means of the Szilard-Chalmers effect from potassium chromate irradiated at low temperature. By D. Brune. 1967. 15 p. Sw. cr. 10:–.

292. Total and differential efficiencies for a circular detector viewing a circular radiator of finite thickness. By A. Lauber and B. Tollander. 1967. 45 p. Sw cr 10:–.

293. Absolute M1 and E2 transition probabilities in ^{233}U By S. G. Malmskog and M. Höjeberg. 1967. 37 p. Sw. cr. 10:–.

294. Cerenkov detectors for fission product monitoring in reactor coolant water. By O. Strindehag. 1967 56 p. Sw. cr 10:–

295. RPC calculations for K-forbidden transitions in ^{183}W. Evidence for large inertial parameter connected with high-lying rotational bands. By S. G Malmskog and S. Wahlborn. 1967. 25 p. Sw. cr. 10:–.

296. An investigation of trace elements in marine and lacustrine deposits by means of a neutron activation method. By O. Landström, K. Samsahl and C-G. Wenner. 1967. 40 p. Sw. cr. 10:–.

297. Natural circulation with boiling By R. P. Mathisen. 1967. 58 p. Sw. cr. 10:–.

298. Irradiation effects at 160–240°C in some Swedish pressure vessel steels. By M Grounes, H. P. Myers and N-E. Hannerz. 1967. 36 p. Sw. cr. 10:–.

299. The measurement of epithermal-to-thermal U-238 neutron capture rate (ρ_{28}) in Ågesta power reactor fuel. By G. Bernander. 1967. 42 p. Sw. cr. 10:–.

300 Levels and transition rates in ^{199}Au. By S. G. Malmskog, A. Bäcklin and B. Fogelberg. 1967. 48 p. Sw cr. 10:–

301. The present status of the half-life measuring equipment and technique at Studsvik. By S. G. Malmskog. 1967. 26 p. Sw. cr. 10:–.

302. Determination of oxygen in aluminum by means of 14 MeV neutrons with an account of flux attenuation in the sample. By D. Brune and K. Jirlow 1967. 16 p. Sw. cr. 10:–

303. Neutron elastic scattering cross sections of the elements Ni, Co, and Cu between 1.5 and 8.0 mev. By B. Holmqvist and T. Wiedling. 1967. 17 p Sw. cr. 10:–.

304. A study of the energy dependence of the Th232 capture cross section in the energy region 0.1 to 3.4 eV. By G. Lundgren. 1967. 25 p. Sw. cr. 10:–.

305 Studies of the reactivity effect of polythene in the fast reactor FRO. By L. I. Tirén and R. Håkansson. 1967. 25 p. Sw. cr. 10:–.

306. Final report on IFA-10, the first Swedish instrumented fuel assembly irradiated in HBWR, Norway. By J-Å. Gyllander. 1967. 35 p. Sw. cr. 10:–.

307. Solution of large systems of linear equations with quadratic or non-quadratic matrices and deconvolution of spectra. By K. Nygaard. 1967. 15 p. Sw. cr. 10:–.

308. Irradiation of superheater test fuel elements in the steam loop of the R2 reactor. By F. Ravndal. 1967. 94 p. Sw. cr. 10:–.

309. Measurement of the decay of thermal neutrons in water poisoned with the non-1/v neutron absorber cadmium. By. L. G. Larsson and E. Möller. 1967. 20 p. Sw. cr. 10:–.

310. Calculated absolute detection efficiencies of cylindrical NaI (Tl) scintillation crystals for aqueous spherical sources. By. O. Strindehag and B. Tollander. 1968. 18 p. Sw. cr. 10:–.

311. Spectroscopic study of recombination in the early afterglow of a helium plasma. By J. Stevefelt. 1968. 49 p. Sw. cr. 10:–.

312. Report on the personnel dosimetry at AB Atomenergi during 1966. By J. Carlsson and T. Wahlberg. 1968. 10 p. Sw. cr. 10:–.

313. The electron temperature of a partially ionized gas in an electric field. By F. Robben. 1968. 16 p. Sw. cr. 10:–.

314. Activation Doppler measurements on U238 and U235 in some fast reactor spectra. By L. I. Tirén and I. Gustafsson. 1968. 40 p. Sw. cr. 10:–.

315. Transient temperature distribution in a reactor core with cylindrical fuel rods and compressible coolant. By H. Vollmer. 1968. 38 p. Sw. cr. 10:–.

316. Linear dynamics model for steam cooled fast power reactors. By H. Vollmer. 1968. 40 p. Sw. cr. 10:–.

317. A low level radioactivity monitor for aqueous waste. By E. J. M. Quirk. 1968. 35 p. Sw. cr. 10:–.

318. A study of the temperature distribution in UO_2 reactor fuel elements. By I. Devold. 1968. 82 p. Sw. cr. 10:–.

319. An on-line water monitor for low level β-radioactivity measurements. By E. J. M. Quirk. 1968. 26 p. Sw. cr. 10:–.

320. Special cryostats for lithium compensated germanium detectors. By A. Lauber, B. Malmsten and B. Rosencrantz. 1968. 14 p. Sw. cr. 10:–.

321. Stability of a steam cooled fast power reactor, its transients due to moderate perturbations and accidents. By H. Vollmer. 1968. 36 p. Sw. cr. 10:–.

322. Progress report 1967. Nuclear chemistry. 1968. 30 p. Sw. cr. 10:–.

323 Noise in the measurement of light with photomultipliers. By F. Robben. 1968. 74 p. Sw. cr. 10:–.

324. Theoretical investigation of an electrogasdynamic generator. By S. Palmgren. 1968. 36 p. Sw. cr. 10:–.

325. Some comparisons of measured and predicted primary radiation levels in the Ågesta power plant. By E. Aalto, R Sandlin and Å. Krell. 1968. 44 p. Sw. cr. 10:–.

326. An investigation of an irradiated fuel pin by measurement of the production of fast neutrons in a thermal column and by pile oscillation technique. By Veine Gustavsson. 1968 24 p. Sw. cr. 10:–.

327. Phytoplankton from Tvären, a bay of the Baltic, 1961–1963. By Torbjörn Willén. 1968. 76 p. Sw. 10:–.

328. Electronic contributions to the phonon damping in metals. By Rune Jonson. 1968. 38 p. Sw cr. 10:–.

329. Calculation of resonance interaction effects using a rational approximation to the symmetric resonance line shape function. By H. Häggblom. 1968. 48 p. Sw. cr. 10:–.

330. Studies of the effect of heavy water in the fast reactor FR0. By L. I. Tirén, R. Håkansson and B. Karmhag. 1968. 26 p. Sw. cr. 10:–.

331. A comparison of theoretical and experimental values of the activation Doppler effect in some fast reactor spectra By H. Häggblom and L. I. Tirén. 1968. 28 p. Sw. cr. 10:–.

332. Aspects of low temperature irradiation in neutron activation analysis. By D. Brune. 1968. 12 p. Sw. cr. 10.–.

333. Application of a betatron in photonuclear activation analysis. By D. Brune, S. Mattsson and K. Lidén. 1968. 13 p. Sw. cr. 10:–.

334. Computation of resonance-screened cross section by the Dorix-Speng system. By H. Häggblom. 1968. 34 p. Sw. cr. 10:–.

335. Solution of large systems of linear equations in the presence of errors. A constructive criticism of the least squares method. By K. Nygaard. 1968. 28 p. Sw. cr. 10:–.

336. Calculation of void volume fraction in the subcooled and quality boiling regions. By S. Z. Rouhani and E. Axelsson. 1968. 26 p. Sw. cr. 10:–.

337. Neutron elastic scattering cross sections of iron and zinc in the energy region 2.5 to 8.1 MeV. By B. Holmqvist, S. G. Johansson, A. Kiss, G. Lodin and T. Wiedling. 1968. 30 p. Sw. cr. 10:–.

338. Calibration experiments with a DISA hot-wire anemometer. By B. Kjellström and S. Hedberg. 1968. 112 p. Sw. cr. 10:–.

339. Silicon diode dosimeter for fast neutrons. By L. Svansson, P. Swedberg, C-O. Widell and M. Wik. 1968. 42 p. Sw. cr. 10:–.

340. Phase diagrams of some sodium and potassium salts in light and heavy water. By K. E. Holmberg. 1968 48 p. Sw. cr. 10:–.

341. Nonlinear dynamic model of power plants with single-phase coolant reactors. By H. Vollmer. 1968. 26 p. Sw. cr. 10:–.

342. Report on the personnel dosimetry at AB Atomenergi during 1967. By J. Carlsson and T. Wahlberg. 1968. 10 p. Sw. cr. 10:–.

343. Friction factors in rough rod bundles estimated from experiments in partially rough annuli – effects of dissimilarities in the shear stress and turbulence distributions. By B. Kjellström. 1968. 22 p. Sw. cr. 10:–.

344. A study of the resonance interaction effect between ^{238}U and ^{239}Pu in the lower energy region. By H. Häggblom. 1968. 48 p. Sw. cr. 10:–.

345. Application of the microwave discharge modification of the Wilzbach technique for the tritium labelling of some organics of biological interest. By T. Gosztonyi. 1968. 12 p. Sw. cr. 10:–.

346. A comparison between effective cross section calculations using the intermediate resonance approximation and more exact methods. By H. Häggblom. 1969. 64 p. Sw. cr. 10:–.

347. A parameter study of large fast reactor nuclear explosion accidents. By J. R. Wiesel. 1969. 34 p. Sw. cr. 10:–.

348. Computer program for inelastic neutron scattering by an anharmonic crystal. By L. Bohlin, I. Ebbsjö and T. Högberg. 1969. 52 p. Sw. cr. 10:–.

349. On low energy levels in ^{185}W. By S. G. Malmskog, M. Höjeberg and V. Berg. 1969. 18 p. Sw. cr. 10:–.

350. Formation of negative metal ions in a field-free plasma. By E. Larsson. 1969. 32 p. Sw. cr. 10:–.

351. A determination of the 2 200 m/s absorption cross section and resonance integral of arsenic by pile oscillator technique. By E. K. Sokolowski and R. Bladh. 1969. 14 p. Sw. cr. 10:–.

352. The decay of ^{191}Os. By S. G. Malmskog and A. Bäcklin. 1969. 24 p. Sw. cr. 10:–.

353. Diffusion from a ground level point source experiment with thermoluminescence dosimeters and Kr 85 as tracer substance. By Ch. Gyllander, S. Hollman and U. Widemo. 1969. 23 p. Sw. cr. 10:–.

354. Progress report, FFN, october 1, 1967 – september 30, 1968. By T. Wiedling. 1969. 35 p. Sw. cr. 10:–.

355. Thermodynamic analysis of a supercritical mercury power cycle. By A. S. Roberts, Jr., 1969. 25 p. Sw. cr. 10:–.

List of published AES-reports (In Swedish)

1. Analysis be means of gamma spectrometry. By D. Brune. 1961. 10 p. Sw. cr. 6:–.
2. Irradiation changes and neutron atmosphere in reactor pressure vessels-some points of view. By M. Grounes. 1962. 33 p. Sw. cr. 6:–.
3. Study of the elongation limit in mild steel. By G. Östberg and R. Attermo. 1963. 17 p. Sw. cr. 6:–.
4. Technical purchasing in the reactor field. By Erik Jonson. 1963. 64 p. Sw. cr. 8:–.
5. Ågesta nuclear power station. Summary of technical data, descriptions, etc. for the reactor. By B. Lilliehöök. 1964. 336 p. Sw. cr. 15:–.
6. Atom Day 1965. Summary of lectures and discussions. By S. Sandström. 1966. 321 p. Sw. cr. 15:–.
7. Building materials containing radium considered from the radiation protection point of view. By Stig O. W. Bergström and Tor Wahlberg. 1967. 26 p. Sw. cr. 10:–.

Additional copies available from the library of AB Atomenergi, Fack, S-611 01 Nyköping, Sweden.

EOS-tryckerierna, Stockholm 1969